PHOTOMETRIC OBSERVATIONS OF ECLIPSING BINARY GO CYG

Alexandre Barbosa, Diogo Miguez, Rita Santos, Tomás Mendes

Departamento de Física, Instituto Superior Técnico (Universidade de Lisboa)
alexandre.barbosa@tecnico.ulisboa.pt diogomiguez@tecnico.ulisboa.pt
ritapsantos@tecnico.ulisboa.pt tomaslmendes@tecnico.ulisboa.pt

November 29, 2022

ABSTRACT

Observations of the Binary System GO Cygni are presented, covering instances of both primary and secondary eclipes throughout the course of four nights in clear, B, V and R filters. We estimate the orbital period as $T = 0.717^{+0.003}_{-0.002}$ days, through a Lomb-Scargle Periodogram. Optical light curves and new times of minima are obtained. We study the orbital period variation since 1930 through an observed-minus-calculated (O-C) diagram and find evidence for the presence of a third body in the orbit, with a period of around 122 years, but we do not rule out a mechanism of mass transfer between the primary and secondary components as an explanation for the orbital period increase, at a rate of $dP/dt = 5.87 \times 10^{-8}$ days/year.

1 INTRODUCTION

A binary stellar system is composed of two gravitationally bound stars that orbit around a common centre of mass. Current estimates indicate that around a third of the stars in the galaxy form binary or higher-multiple systems [1], including up to three-quarters of visible stars [2] and a majority of massive stars, accounting for over half of main-sequence stars with M > $1.5M_{\odot}$ and over 80% of those with M $\geq 16M_{\odot}$. [3]

In an eclipsing binary system, the orbital plane contains the line of sight of an observer on Earth and the stars periodically eclipse each other, so that the observed brightness of the system from their perspective varies accordingly. Although the light of individual components does not vary, these are variable stars due to the eclipses, with periodic light curves.

GO Cyg is a β Lyrae-type (EB) binary system located in the Cygnus Constellation, with an orbital period of 0^d71 and an apparent magnitude of 8.47 [4]. An EB binary customarily has heavy giant or supergiant components of early spectral types (B-A), and nearly two thousand have already been catalogued (around 3% of all classified variable stars). [5]

In this type of binary systems, the two stars are sufficiently close to each other that the strong gravitational pull warps each of them into an ellipsoidal shape and can lead to the creation of an accretion disk [6]. GO Cyg is such an ellipsoidal system; thus, the light curves are expected to show a continuously varying brightness, rather than a steep change during the eclipse, with observable secondary minima.

After more than ninety years of observations [7], GO Cyg is widely reported to have a filled primary Roche lobe (the surface wherein the orbiting material is bound by gravity to that star), and an almost filled secondary Roche lobe, therefore classifying as a close, semi-detached binary system. [8]

In a semi-detached binary, tracking orbital period changes can provide evidence for mass transfer between the primary and secondary stars (and vice-versa), magnetic activity, or the existence of a third body in the orbit [8].

An observed-minus-calculated (O-C) diagram compares the observed and calculated time of an astronomical event (here, the mid-eclipse), and through the resulting curve subtle changes in periodicity can be precisely measured. [6]

A number of estimates is available in the literature for the orbital increase of GO Cyg, ranging from Q = 7×10^{-11} to Q = $1.6(\pm 2) \times 10^{-10}$ days [9] [10] using a quadratic fit

$$T_{min} = T_0 + P \times E + Q \times E^2 \tag{1}$$

where T_{min} are the times of minima, T_0 is a reference epoch, E is the number of cycles since T_0 and P denotes the period.

An increase of $dP/dt = 1.28 \times 10^{-7}$ to 1.51×10^{-7} d/yr has thus been found for GO Cyg [11][12], at odds with a reported period decrease of $dP/dt = -1.4 \times 10^{-9}$ d/yr obtained in [8] from the analysis of light curves since 1950, which from 1934 to 1984 may be attributable to a magnetic cycle [13].

Additionally, from analysis of light curves, the separation, mass, radii and luminosity of both components of GO Cyg have been estimated [8]. However, no reliable radial velocity measurements for this system can be found in the literature.

Moreover, the existence of a third body with a mass of 0.6 $M_{\odot}$ and a period of around 90 yrs has been advanced as an explanation for this variation [14], supported by fitting a sinusoidal variation in the O-C curve, instead of a parabola.

Although the system has been extensively studied, conflicting results and explanations abound for its period variation, and we hope that the additional present-epoch data we obtained is useful to ultimately settle these longstanding questions.

The paper is organised as follows: the photometric observations are presented in Section 2, in which we discuss the methods used for data processing. The analysis of the processed data is done in Section 3, where we estimate the orbital period, the light curves for each band are presented and discussed, and a study on the period variation is performed using data from previous studies and our own estimated minima.

2 Observations and Data Handling

The data used in this paper was obtained in four nights between the 26th and the 29th September 2022. The observations were carried out at CIGeoE - Centro de Informação Geoespacial do Exército (Lisboa, Portugal, Latitude 38.77806N, Longitude -9.11367E) with a Celestron 14" Shmidt-Cassegrain telescope, which has a 356 mm aperture and a 3910 mm focal length. Using a Moravian G2-1600 CCD we observed GO Cyg through clear, B ($\lambda_B = 445nm$),V ($\lambda_V = 551nm$) and R ($\lambda_R = 658nm$) filters (Johnson system), applying different integration times of 10s, 25s, 20s, and 10s, respectively, in order to maximize the counts on the CCD.

The motion and calibration of the telescope was done using the Celestron PWI Telescope Control software and the CCD images were processed with DS9. This data was subsequently reduced and analysed with the `Astropy` Python package; the code is available on Supplementary Materials section.

All the data obtained with the CCD needs to be reduced before any analysis can be done. Furthermore, it inevitably contains noise from different sources which must be accounted for from the start, since it propagates through every function we applied to the data. Sources of noise from the CCD include *read-out noise* (constant), noise due to *dark currents* (disregarded since we kept the CCD at T=-20ºC during observations) and statistical fluctuations (assumed to be *Poisson-distributed*, $\sim \sqrt{N}$).

2.1 Data Reduction

We began each observation session by taking roughly 50 bias shots (with a closed shutter and zero exposure time). We obtained the master bais as the median of the bias shots (fig. 1), which was subtracted from all subsequent shots, effectively getting rid of the bias offset of the CCD and also to get a standard deviation of the bias level counts which, multiplied by the gain of the CCD (1.5 e^-/ADU), gives the read-out error.

In each session we also took around 70 flat shots of a source of continuous light (the sky twilight) in all filters, which required different exposure times. These expose effects characteristic of the CCD such as vignetting, pixel manufacturing differences and dust grains on optical elements. For each flat shot we subtract the master bias, and then divide it by the median of the counts. We then take the median of all flat shots taken

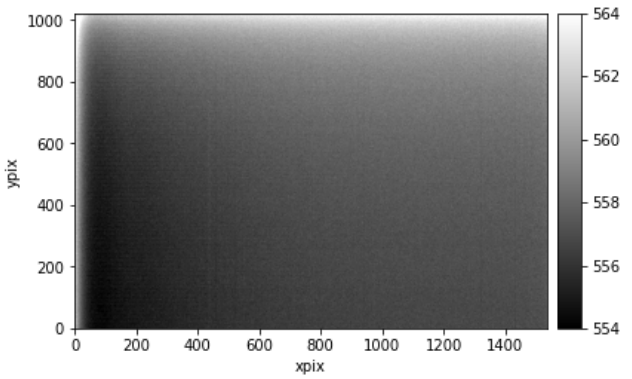

Figure 1: Master Bias obtained for all observing sessions.

with a certain filter to get a master flat for each filter. The masterflat for a clear filter is shown in fig. 2. We applied the standard data reduction formula (2) to every science shot we took throughout the observing sessions.

$$\text{Reduced Data} = \frac{\text{Image - Masterbias}}{\text{Masterflat}} \tag{2}$$

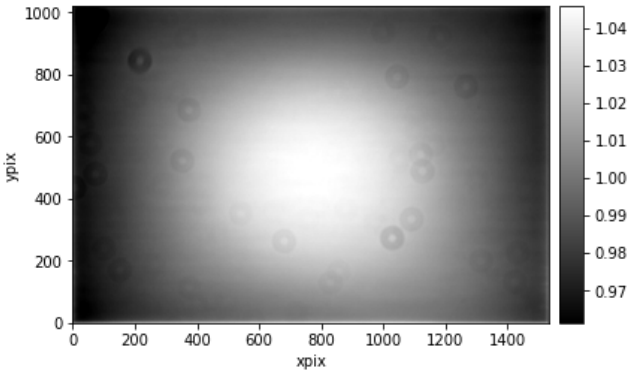

Figure 2: Master Flat for a clear filter for all sessions.

2.2 Data Preparation

After reducing the data, we took further steps to prepare the data in order to obtain light curves for GO Cyg, starting by the removal of the background. To estimate the background count levels for each shot, the Python package `Photutils` was used, where a light source was considered a stellar object, and hence discarded, for levels of counts more than 3σ away from the computed median (3σ-*clipping*). The resulting background shots were subsequently subtracted to all the data.

We proceeded by aligning the shots for each filter using the Python module `Astroalign`.

The `DAOStarFinder` function from `Photutils` was used in order to detect the stars in the reduced data. This function

searches for maxima in the data that follow a 2D Gaussian with an inputed FWHM. We estimated the FWHM for each filter by fitting a 2D Gaussian to the data (Table 2.2).

Clear	Blue	Red	Green
9.24 ± 0.12	9.25 ± 0.48	9.29 ± 1.61	9.24 ± 1.98

Table 1: Calculated FWHM values (px) for each filter

The magnitude of GO Cyg and three close stars (labeled A, B and C for simplicity — see Figure 3) was also computed with `DAOStarFinder`. Since we aim to do differential photometry with GO Cyg and these other stars, we only care about differences of magnitude, which makes the apparent magnitude given by this function adequate. The errors of the magnitudes were estimated by taking the absolute difference between these and the magnitudes found when inputting $FWHM - \sigma_{FWHM}$ in `DAOStarFinder`. The computed magnitudes for $FWHM + \sigma_{FWHM}$ were not taken into account since with the larger FWHM the finder function would malfunction.

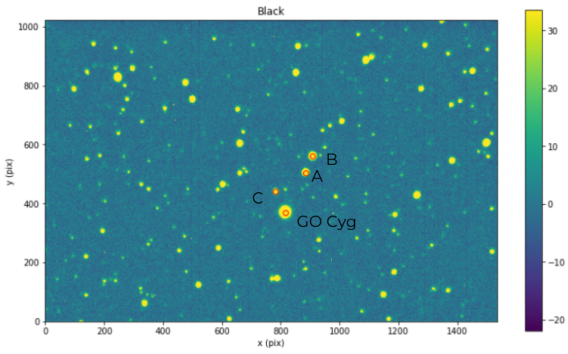

Figure 3: Stars Identified for Differential Photometry

2.3 Differential Photometry

In differential photometry, we're interested in measuring the difference in brightness of different objects. In this study, we want to see how the magnitude of GO Cyg changes in relation to other stars in the same Field of View. We chose to analyse the aforementioned stars A, B and C as candidates for differential photometry. We inspect the magnitude of each of these stars as a function of time to make sure they aren't variable stars at least in the time frame of our observations), as plotted in Figure 4. As we can see, the magnitude of A, B and C are constant in time, which makes them good targets for differential photometry, and from now on we take the average of magnitude of these three stars in each picture and subtract it to the magnitude of our target GO Cyg, to study how it varies.

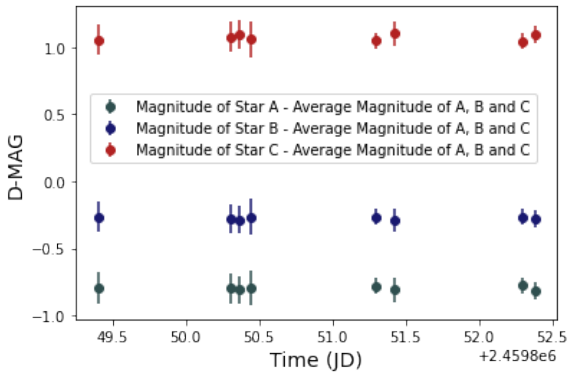

Figure 4: Difference between individual and average magnitudes for stars A, B and C, with a clear filter.

Finally, we stack equivalent shots, i.e. combine the science images taken with the same filter at aproximmately the same time. We perform this by averaging the magnitudes the epochs of images that were taken in sequence for each filter.

	GO Cyg	A	B	C
Clear	(815, 369)	(884, 504)	(908, 560)	(783, 439)
Blue	(817,369)	(886, 503)	(910, 558)	(785, 438)
Red	(822, 356)	(891, 490)	(915, 545)	(789, 426)
Green	(822, 359)	(891, 493)	(915, 549)	(790, 429)

Table 2: Coordinates of GO Cyg and stars A, B, C used for differential photometry within the CCD (px).

2.4 Ephemeris

We used the linear ephemeris by Purgathofer and Prochazka (1967) [15] for data reduction and analysis.

$$T_{min} = 2433930.40561 + 0.71776382 \times E, \qquad (3)$$

where E is the number of cycles since the reference epoch T_0 = 2433930.40561 JD (10-10-1951).

3 Results

3.1 Period Estimation

We use a Lomb-Scargle periodogram to detect the periodic signals in our data, since our observations are unevenly spaced.

Only the data with no filter is used to estimate the period, due to the high relative errors of the data in the B, V and R bands.

Our periodogram was computed using the `LombScargle` method implemented in `Astropy.Timeseries` [16].

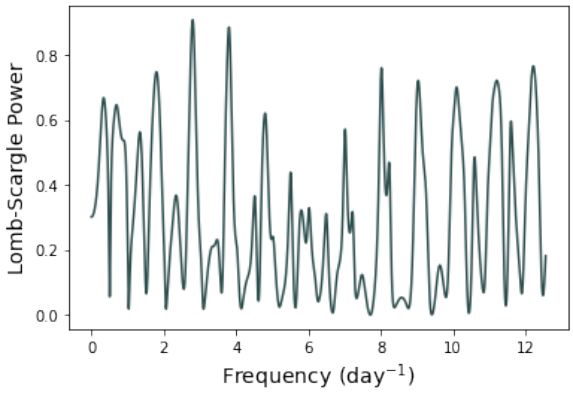

Figure 5: Lomb-Scargle Periodogram for GO Cyg (Clear)

We note that the highest-power peak corresponds to *twice* the orbital frequency, since two eclipses and hence two brightness minima, with similiar depths, occur in each orbit. We therefore estimate the orbital period as

$$T = 0.717^{+0.003}_{-0.002} \text{ days}$$

where the uncertainty bands are estimated by varying the sampling rate between 5 and 1000 samples per peak, and the false alarm probability (i.e, the probability of finding a peak with at least a given height assuming the data is Gaussian noise) [17] for the highest-power peak is estimated at of 1.14×10^{-34}.

Despite the low observation frequency, this statistic gives a strong indication that the periodic signal is present in our data.

Our estimated orbital period is in full agreement with more precise measurements found in literature [8], where

$$T = 0.717764585 \pm 0.000000015 \text{ days}$$

In addition to the peaks we expect to observe (multiples of the orbital frequency, since the light-curve for β-Lyr systems is not a perfect sinusoid), we also notice a leakage of power from the expected peaks due to the measurement uncertainties (which are accounted for, assuming a gaussian distribution).

Additionally, since our observations take place only at night, there are aliases with non-negligible power at frequencies:

$$f_{alias} \approx f + n f_{obs} \text{ for } n \in \mathbb{N} \quad (4)$$

where f_{obs} is the observation frequency of one cycle per day.

We note that these aliases correspond to most of the higher-power, evenly spaced peaks in the above plot. [17]

3.2 Light Curves and Phase Diagrams

3.2.1 Clear

We present the observed light curve for GO Cyg with a clear filter in figure 6, where the data points (black error-bars) were fitted by the least-squares method to the Fourier series

$$\text{D-MAG} = \theta_0 + \sum_{n=1}^{2} \theta_{2n-1} \sin(2n\pi f t) + \theta_{2n} \cos(2n\pi f t)$$

where f is the orbital frequency (inverse of the previously determined period, using the `LombScargle` method).

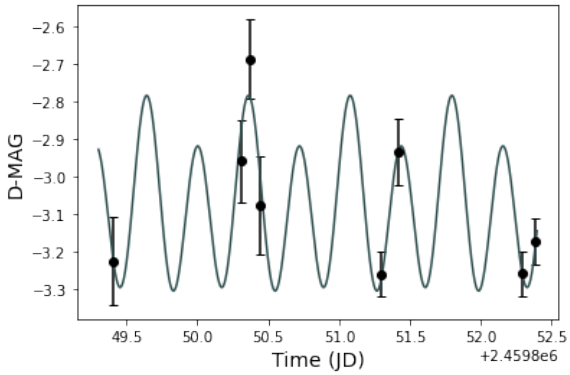

Figure 6: Observed Light Curve of GO Cyg (clear filter), differential magnitude (D-MAG) as a function of time (JD).

We present the model parameters in table 3. To estimate the parameter uncertainties, we performed `N = 1000` Monte-Carlo simulations where we added noise drawn from a gaussian distribution centered around the data with standard deviation given by the estimated uncertainty, and fit to the same model.

θ_0	θ_1	θ_2	θ_3	θ_4
$0.062^{+0.015}_{-0.016}$	$0.0059^{+0.044}_{-0.042}$	$0.067^{+0.044}_{-0.050}$	$0.068^{+0.043}_{-0.057}$	$0.21^{+0.043}_{-0.043}$

Table 3: Parameters of the Light-Curve fit to data for GO-Cyg in the clear band, and estimated standard deviations.

We combine the observations from the different nights of observation in the phase diagram plotted in figure 7.

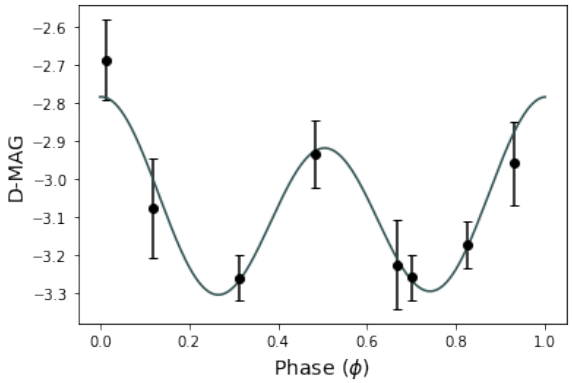

Figure 7: Phase Diagram for Observations of GO Cyg (clear filter) with a CCD camera from 26-09-2022 to 29-09-2022.

Although the number of samples is reduced, care was taken to obtain points close to both the (predicted) primary and secondary eclipse to better estimate of the times of minima.

3.2.2 B-Band

In figure 8, we plot the observed light curve for GO Cyg in the B band, where the data were fitted to the Fourier series with the estimated orbital period using the same method.

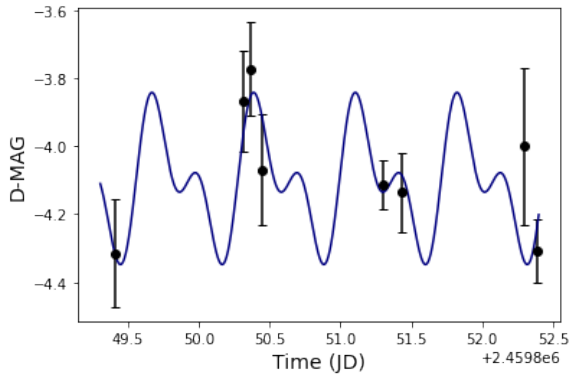

Figure 8: Observed Light Curve of GO Cyg (B filter), differential magnitude (D-MAG) as a function of time (JD).

θ_0	θ_1	θ_2	θ_3	θ_4
$0.013^{+0.021}_{-0.022}$	$0.013^{+0.06}_{-0.06}$	$0.10^{+0.07}_{-0.06}$	$0.052^{+0.062}_{-0.066}$	$0.12^{+0.07}_{-0.07}$

Table 4: Parameters of the Light-Curve fit to data for GO-Cyg in the B band, and estimated standard deviations

Once more, we plot the phase diagram in the B band to combine the observations from different nights, in figure 11.

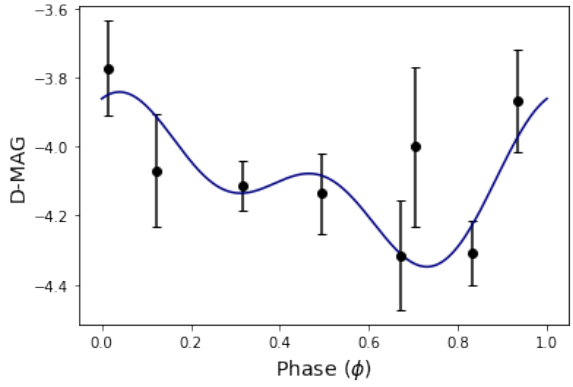

Figure 9: Phase Diagram for Observations of GO Cyg (B filter) with a CCD camera from 26-09-2022 to 29-09-2022.

An analysis of figure 9 suggests an assymetry in the light-curve in the B-band, suggesting a difference in the luminosity of the binary components in this band. However, due to the high uncertainty of the fit parameters, this assymetry, also reported in [9] for the 0.6-0.7 orbital phase (but no evidence of which was found in [8]), cannot be definitely estabilished.

3.2.3 R-Band

We present also the observed light curve for GO Cyg in the R band, where the points were similiarly fitted to a Fourier series with the previously determined orbital frequency.

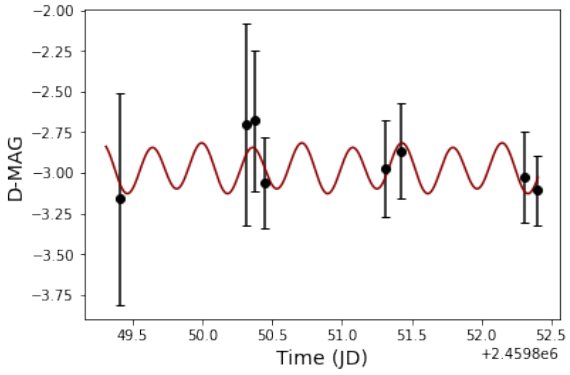

Figure 10: Observed Light Curve of GO Cyg (R filter), differential magnitude (D-MAG) as a function of time (JD).

We note that, although the light curve intersects the error bars of all data points, the uncertainties are very large, likely due to lower contrast in the obtained images, a consequence of the lower average number of counts in the data.

Hence, the model parameters in table 5, that correspond to the amplitude of different modes, cannot be taken as reliable estimates, since none is larger than their standard deviation, calculated from `N=5000` Monte-Carlo simulations.

θ_0	θ_1	θ_2	θ_3	θ_4
$0.02^{+0.04}_{-0.04}$	$0.02^{+0.18}_{-0.16}$	$-0.01^{+0.16}_{-0.18}$	$0.03^{+0.17}_{-0.16}$	$0.14^{+0.18}_{-0.18}$

Table 5: Parameters of the Light-Curve fit to data for GO-Cyg in the R band, and estimated standard deviations.

Again, we plot the phase diagram in the R band to combine the observations from different nights, in figure 11.

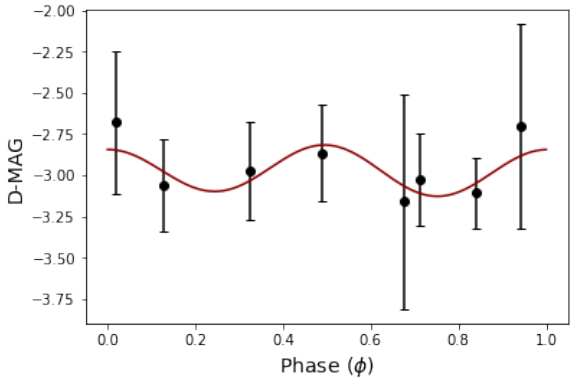

Figure 11: Phase Diagram for Observations of GO Cyg (R filter) with a CCD camera from 26-09-2022 to 29-09-2022.

3.2.4 V-Band

Finally, in figure 12, we present the observed light curve for GO Cyg in the V band, where the points were once again fitted to the same model with the determined orbital frequency.

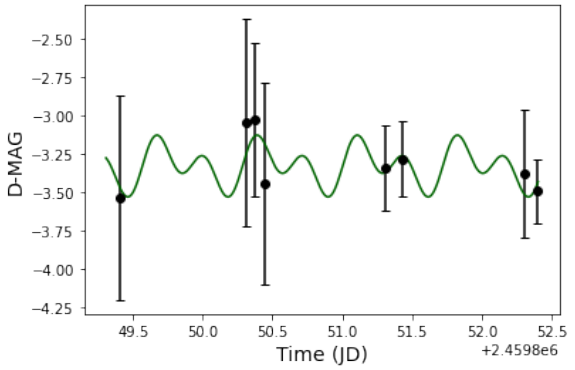

Figure 12: Observed Light Curve of GO Cyg (V filter), differential magnitude (D-MAG) as a function of time (JD).

Our model suggests that the light curve is assymetric, similiarly to the case for the B-band. However, since the standard deviation of the fit parameters shown in table 6 (estimated as before from `N = 5000` Monte Carlo simulations) is significantly larger than the parameters themselves, no conclusions can be reasonably inferred about the luminosity of the binary components across different bands from our data.

θ_0	θ_1	θ_2	θ_3	θ_4
$0.036^{+0.099}_{-0.096}$	$0.082^{+0.20}_{-0.20}$	$0.04^{+0.19}_{-0.19}$	$0.01^{+0.20}_{-0.20}$	$0.11^{+0.20}_{-0.21}$

Table 6: Parameters of the Light-Curve fit to data for GO-Cyg in the V band, and estimated standard deviations.

We also plot the phase diagram for this band in figure 13.

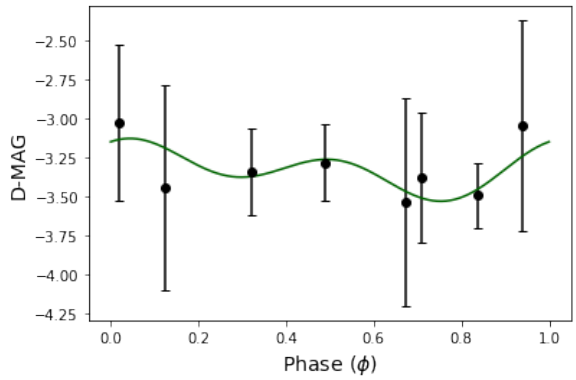

Figure 13: Phase Diagram for Observations of GO Cyg (V filter) with a CCD camera from 26-09-2022 to 29-09-2022.

3.3 Period Variation

A number of studies [9, 10, 11, 12, 18] have shown that the period of the GO Cyg system is slightly increasing. However, in some intervals, it has been found by [8, 13] that the orbital period of GO Cygni is, in fact, decreasing.

We combined our observations with previous measurements since 1930 (listed in [11]) and plotted an O-C (Observed-Computed) curve for the times of minima.

We started by converting our observations to Heliocentric Julian Date (HJD) to correct for differences in the Earth's position with respect to the Sun and then obtained the following times of minima from the light curves.

Min	1	2	3	4	5
T_{min}	2459849.6421	2459850.3599	2459851.0776	2459851.7954	2459852.5132

Table 7: Estimated times of minima in Heliocentric Julian Date (HJD) from the light-curves.

In the dataset collected by [11], no errors are provided for the observed-calculated minima, so no estimates for standard deviation of our results in this section are computed.

Finally, we plotted $T^{obs}_{min} - T^{calc}_{min}$ against E (integer number of cycles), shown in Fig.14, and performed a quadratic fit, obtaining

$$T_{min} = 2433930.413 + 0.7177641E + 5.9841093 \times 10^{-11} E^2, \quad (5)$$

corresponding to a period increase of

$$\frac{dP}{dt} = 5.87 \times 10^{-8} \text{ days/year.}$$

The quadratic term obtained is not included in the interval of values indicated in section 1. In fact it is 14.5% smaller than the lower value encountered in the literature [18].

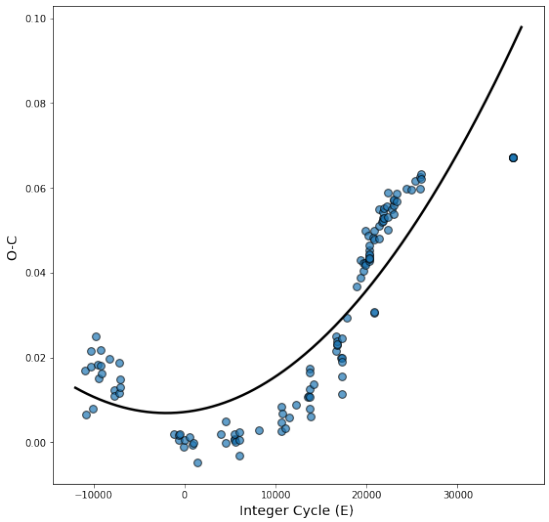

Figure 14: O-C diagram of GO Cyg with quadratic fit. To obtain this plot, our own data was used (corresponding to the data points in the right), as well as data collected by [11]

The parabola shape for the change of the period possibly indicates mass transfer between primary and secundary stars.

Another hypothesis is the existence of a third body orbiting the system, hence changing the binary's period. This can be modeled with a sinusiodal model due to [19].

We fitted the data to a generalized sinusoidal function of the form $a\sin(bE+c)+d$, plotted in figure 15, obtaining the parameters in table 3.3.

Parameter	Value
a	0.0384859
b	0.0001009
c	-1.8153914
d	0.0333484

Table 8: Result of the fit of the O-C curve to a generalised sinusoidal function of the form $a\sin(bE+c)+d$

With this expression we obtain a period for the variation of the the times of minima equal to $P_{o-c} = 62242.4$ cycles $\approx$ 122.39 years. This interval can thus be related to the orbital period of the hypothetical third body, presenting a 32.6% difference from the value obtained by [8].

Further physical properties of the third body can be obtained from the fitting parameters. We do not reproduce this cumbersome calculation, which can be found in [8, 20, 19, 21].

Although the hypothesis of the mass transfer between the primary and secondary components for the period increase was discussed in other articles (e.g. [9, 10]), our data, which is distant in time from the data used by these authors, suggests the best fit to the data is not quadratic, and thus seems to contradict this model.

Additionally, it is not clear whether the sinusiodal variation is due to one or more external bodies.

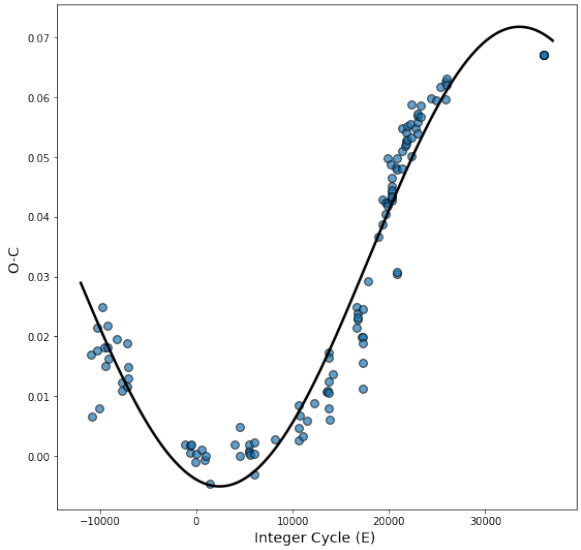

Figure 15: O-C diagram of GO Cyg with sinusoidal fit. To obtain this plot, our own data was used (corresponding to the data points in the right), as well as data collected by [11]

4 Conclusions

We estimated the orbital period of the close eclipsing binary GO Cygni as $T = 0.717^{+0.003}_{-0.002}$ days, in full agreement with more precise estimates found in the literature [4],

We obtain light-curves for GO Cyg in the clear, B, V and R bands for observations from 26-09-2022 to 29-09-2022.

Finally, using data since 1930 in addition to our new times of minima, we study the period variation of GO Cyg, and find evidence supporting the presence of a third body in the orbit with a period of 122.39 years. However, we cannot definitely rule out the hypothesis that the period variation is caused by mass transfer between the two stars.

Over the next decades, precisely monitoring the period of GO Cygni is essential to settle the longstanding debate on the causes of its variation and may be helpful to understand the evolution of close binary systems throughout the universe.

Our results also show that, despite the limitations of using a small telescope in a location with high light-pollution, meaningful data can be obtain for eclipsing binaries with a short orbital period. Hence, amateur astronomers can play an important role on gathering data that may be valuable to astronomy.

5 Supplementary Materials

Python Notebooks used for data analysis.

References

[1] Charles J. Lada. "Stellar Multiplicity and the Initial Mass Function: Most Stars Are Single". In: The Astrophysical Journal 640 (2006), pp. 63–66. DOI: 10.1086/503158.

[2] A. Duquennoy and M. Mayor. "Multiplicity among Solar Type Stars in the Solar Neighbourhood - Part II - Distribution of the Orbital Elements in an Unbiased Sample". In: Astronomy and Astrophysics 248 (1991), p. 485.

[3] Gaspard Duchne and Adam Kraus. "Stellar Multiplicity". In: Annual Review of Astronomy and Astrophysics 51.1 (2013), pp. 269–310. DOI: 10.1146/annurev-astro-081710-102602.

[4] J. M. Kreiner. "Up-to-Date Linear Elements of Eclipsing Binaries". In: Acta Astronomica 54 (2004), pp. 207–210.

[5] N. N. Samus et al. "General catalogue of variable stars: Version GCVS 5.1". In: Astronomy Reports 61.1 (2017), pp. 80–88. DOI: 10.1134/S1063772917010085.

[6] D. Loughney. Eclipsing Binary Observing Guide. London: British Astronomy Association. Retrieved from http://britastro.org/vss/EBHandbook11.pdf. 2011.

[7] H. Schneller. In: Astron. Nachr 235.85 (1928).

[8] B. Ulas et al. "Close binary system GO Cyg". In: New Astronomy 17.3 (2012), pp. 296–302. DOI: 10.1016/j.newast.2011.09.002.

[9] S.M. Zabihinpoor, A. Dariush, and N. Riazi. "Photometric Observation and Period Study of GO Cygni". In: Astrophysics and space Science 302.1 (2006), pp. 27–33.

[10] M.T. Edalati and M. Atighi. "Observations and Light Curves Analysis of Go Cygni". In: Astrophysics and Space Science 253.1 (1997), pp. 107–117. DOI: 10.1023/a:1000532232009.

[11] M. M Elkhateeb. "Variation in the Period of the System GO Cyg". In: Journal of The Korean Astronomical Society 38.1 (2005), pp. 13–16. DOI: 10.1016/j.newast.2011.09.002.

[12] Kyu-Dong Oh et al. "A Photometric Study of EB-type eclipsing binary GO CYG". In: Astrophysics and Space Science 271.3 (2000), pp. 303–320. DOI: 10.1023/a:1002411104173.

[13] Douglas S. Hall and Howard Louth. "New times of minimum and a period study for GO Cygni". In: Journal of Astrophysics and Astronomy 11.3 (1990), pp. 271–275. DOI: 10.1007/bf02709276.

[14] D. Chochol et al. "Light-Time Effect in the Eclipsing Binaries GO Cyg, GW Cep, AR Aur and V505 Sgr". In: Astrophysics and Space Science 304 (2006), pp. 93–96.

[15] A Purgathofer and F Prochazka. "Mitteil". In: Univ. Sternw. Wien 13 (1967), p. 151.

[16] Astropy Time Series: Lomb-Scargle Method. URL: https://docs.astropy.org/en/stable/timeseries/lombscargle.html.

[17] Jacob T. VanderPlas. "Understanding the Lomb-Scargle Periodogram". In: The Astrophys. J. Supplement Series 236.1, 16 (May 2018), p. 16. DOI: 10.3847/1538-4365/aab766. arXiv: 1703.09824 [astro-ph.IM].

[18] B Cester et al. "On the period of the eclipsing binary GO Cygni". In: Acta Astronomica 29 (1979), pp. 433–436.

[19] John B. Irwin. "The Determination of a Light-Time Orbit." In: 116 (July 1952), p. 211. DOI: 10.1086/145604.

[20] John B. Irwin. "Standard light-time curves". In: 64 (May 1959), p. 149. DOI: 10.1086/107913.

[21] Belinda Kalomeni et al. "Absolute Properties of the Binary System BB Pegasi". In: Astronomical Journal 134 (May 2007). DOI: 10.1086/519493.